Supplemental information

Two-state swimming: Strategy and survival of a model bacterial predator in response to environmental cues

Lance W.Q. Xu (徐伟青), J. Shepard Bryan IV, Zeliha Kilic, and Steve Pressé

Two state swimming: strategy and survival of a model bacterial predator in response to environmental cues

Lance W.Q. Xu (徐伟青)[1,2], J. Shepard Bryan IV[1,2], Zeliha Kilic[3], and Steve Pressé[1,2,4,*]

[1]Department of Physics, Arizona State University, Tempe, AZ
[2]Center for Biological Physics, Arizona State University, Tempe, AZ
[3]Single-Molecule Imaging Center, Saint Jude's Children Hospital, Memphis, TN
[4]School of Molecular Sciences, Arizona State University, Tempe, AZ
[*]spresse@asu.edu

SUPPLEMENTARY INFORMATION
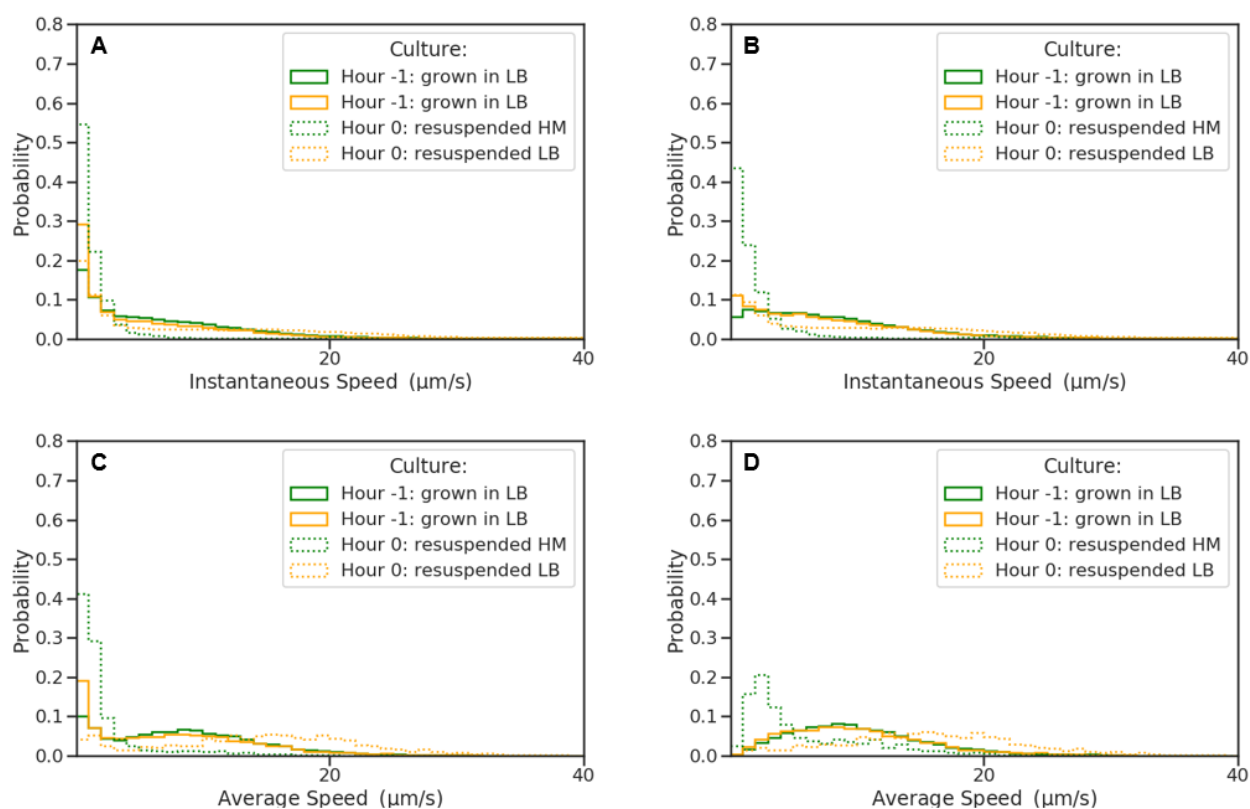
Supplementary Figures

Figure S1: *E. coli* **immediately decreases its speed under starvation conditions.** Two runs were conducted in which each *E. coli* culture was grown in LB (Hour -1) and either resuspended in HM (green) or LB (orange) at Hour 0. (A) The culture resuspended in HM (Hour 0, dotted green) had an increase in population of instantaneous slow speeds as compared to before starvation (Hour -1, solid green). (B) The motile trajectories (at least one instantaneous speed within the trajectory above $5 \, \mu m \, s^{-1}$) of *E. coli* have broader instantaneous speed distributions before centrifugation (Hour -1, solid orange and green) and after resuspension in LB (Hour 0, orange dotted) as compared to the starved culture (Hour 0, dotted green). (C) The culture resuspended in HM (Hour 0, dotted green) had an increase in population of average slow speeds as compared to prior to starvation (Hour -1, solid green) and the culture resuspended in LB (dotted orange). (D) The motile trajectories of *E. coli* have broader average speed distributions before centrifugation (Hour -1, solid orange and green) and after resuspension in LB (Hour 0, orange dotted) as compared to the starved culture (Hour 0, dotted green).
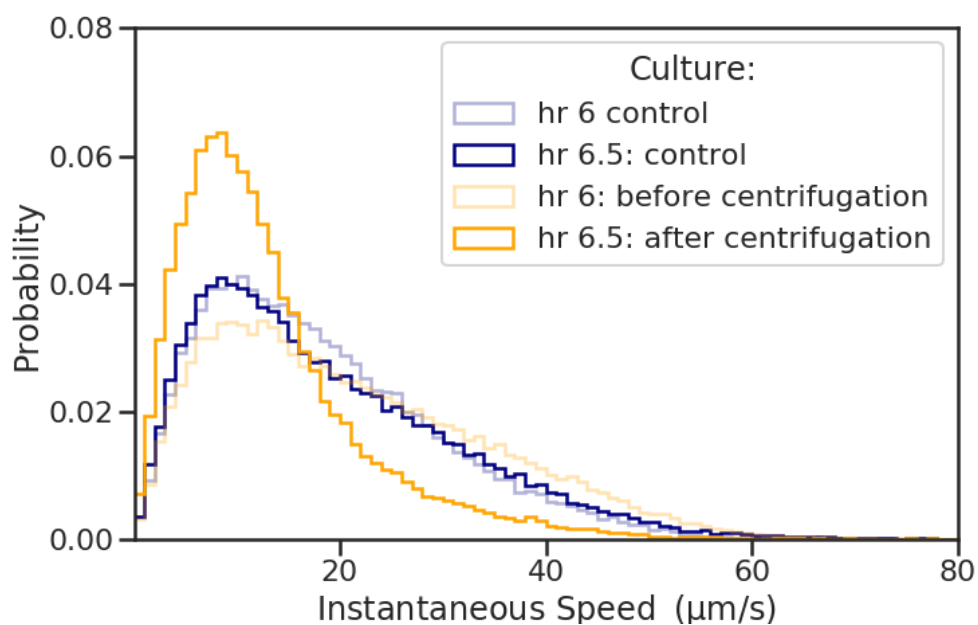
Figure S2: **There is an increase in the apparent diffusive state population after centrifugation.** A *B. bacteriovorus* culture starved for 6 hours was split as seen in the spiking experiments. One culture was not centrifuged (blue) while the other was centrifuged (orange) as discussed in the Methods section. There is no noticeable change between the control (blue) at Hour 6 and Hour 6.5. However, there is an increase in the apparent diffusive population after centrifugation (orange).
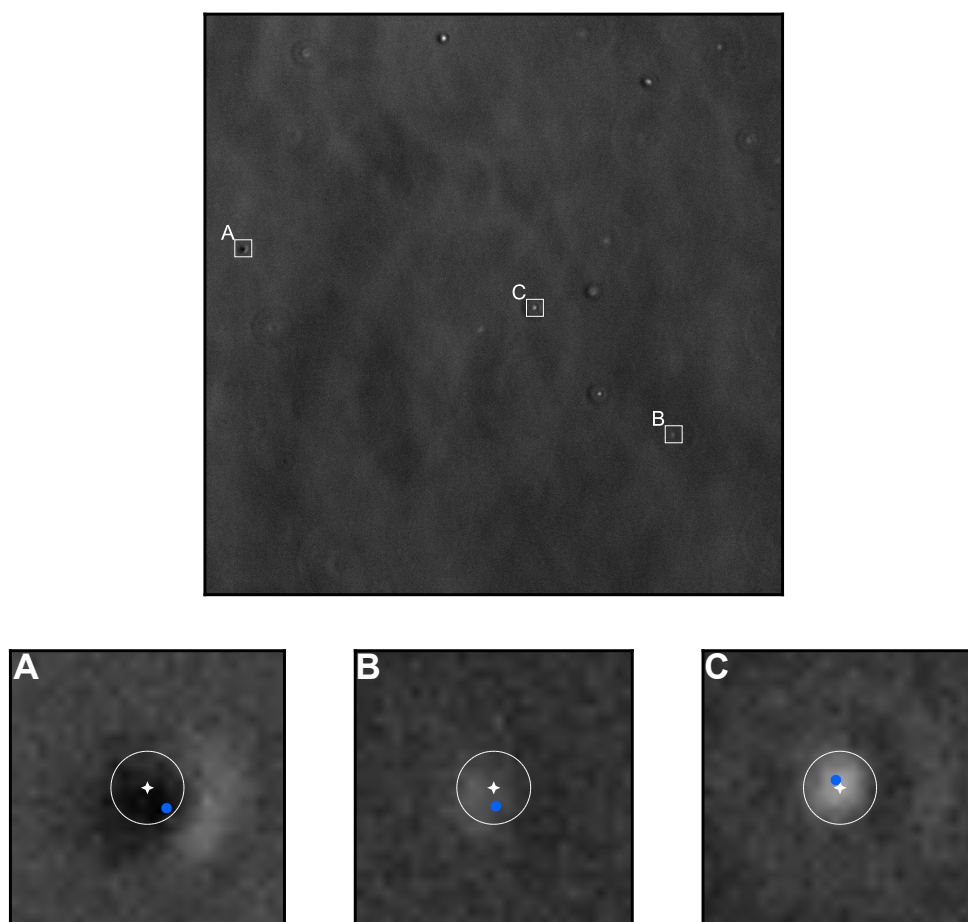
Figure S3: **Localization errors in the analysis of *B. bacteriovorus* datasets.** We selected a frame (1024x1024 pixels, 8 ms) containing multiple *B. bacteriovorus* from inverted phase contrast images. Three 30x30 pixel regions were then selected and presented in panels A-C. The ground truth *B. bacteriovorus* locations, annotated by eye, are denoted by a white star, while the automated (neural net) localization is indicated by a blue dot. The average error between our automated localizations and the hand-annotated localizations across all frames that have been manually annotated is denoted by a circle. The circle's radius represents our localization error.
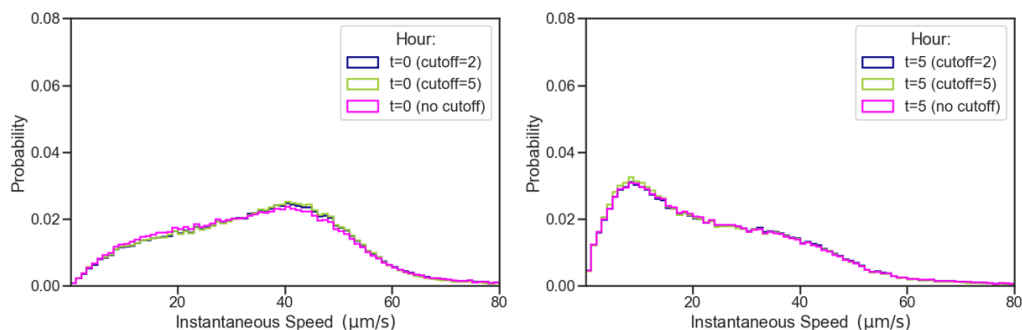
Figure S4: **Varying cutoffs of endpoints of trajectories does not affect the bimodal distribution**. From S1, the relative biases of cutting off different endpoints was seen for Hour 0. However, looking at the distributions after removing these frames from each trajectory, there is no noticeable effect on the structure of the bimodal distributions.
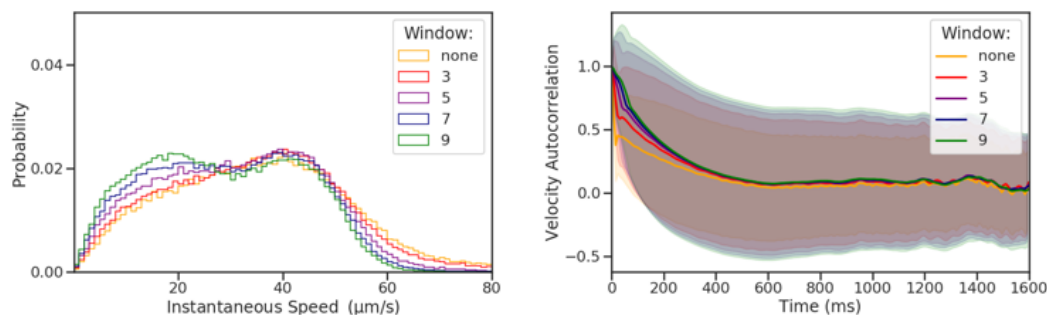

Figure S5: **Using different window averaging has minimal affects on the speed distribution and velocity autocorrelations.** The bimodal distribution for Hour 0 seen in figure 1 was observed using different window averaging. Overall a larger window causes the speed distributions to shift slightly to the left, but the overall distribution shape remains the same. The velocity autocorrelation is very similar regardless of the window. The histogram data was divided into 100 evenly spaced bins.
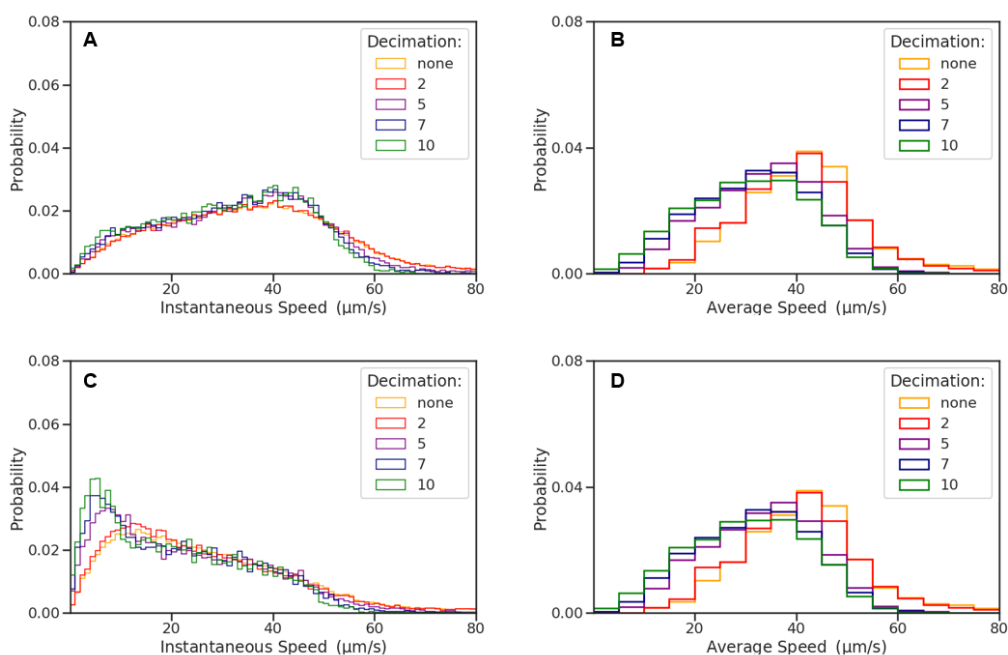
Figure S6: **Decimating the data has minor effects in the speed distributions.** To further test the bimodal behavior seen at early hours of starvation, the data was decimated. For example, for a decimation of 5, every fifth data point of a trajectory was used, thus also decreasing the number of samples. (A) Decimating the data does not show a noticeable effect even as much as taking only every tenth instantaneous speed of a bacterial trajectory at Hour 0. (B) A slight shift to a slower average speed is seen when utilizing fewer data points, but the overall shape of the distribution does not vary greatly at Hour 0. (C) Decimating the data at Hour 5 has an increase in the height of the apparent diffusive peak when taking every fifth to tenth data points. (D) The average speed distributions also show a shift to the left at Hour 5 with larger decimations. As the number of data points is less for Hour 5 compared with Hour 0, this may be a cause for further effects of using larger decimations (fewer data points). All data in the instantaneous speed and average speed histograms was divided into 100 and 30 evenly spaced bins, respectively.
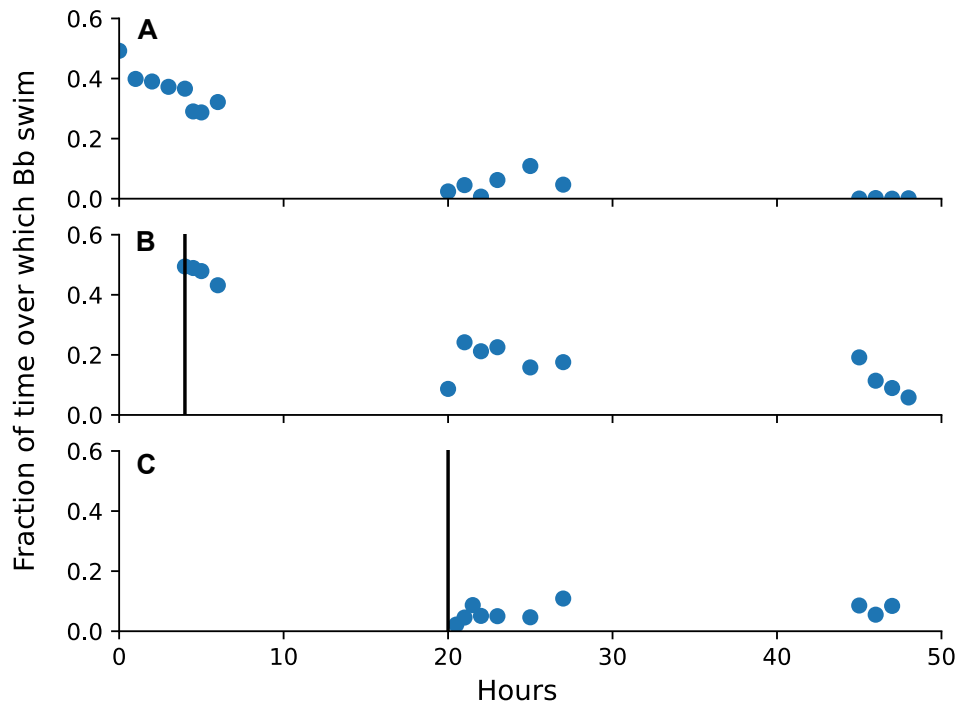
Figure S7: **Fraction of time over which *B. bacteriovorus* swim.** Here we plot the fraction of the *B. bacteriovorus* population swimming over time for our three experiments (no spiking, spiking at Hour 4, and spiking at Hour 20). We determine the fraction of *B. bacteriovorus* that are swimming by thresholding their speeds around 30μm/s, which is the midpoint line between the two speed peaks in figure 1. The top panel shows the control, the middle panel shows the *B. bacteriovorus* that have been spiked at Hour 4, and the bottom panel shows the *B. bacteriovorus* that have been spiked at Hour 20. Black vertical lines represent the spiking time.
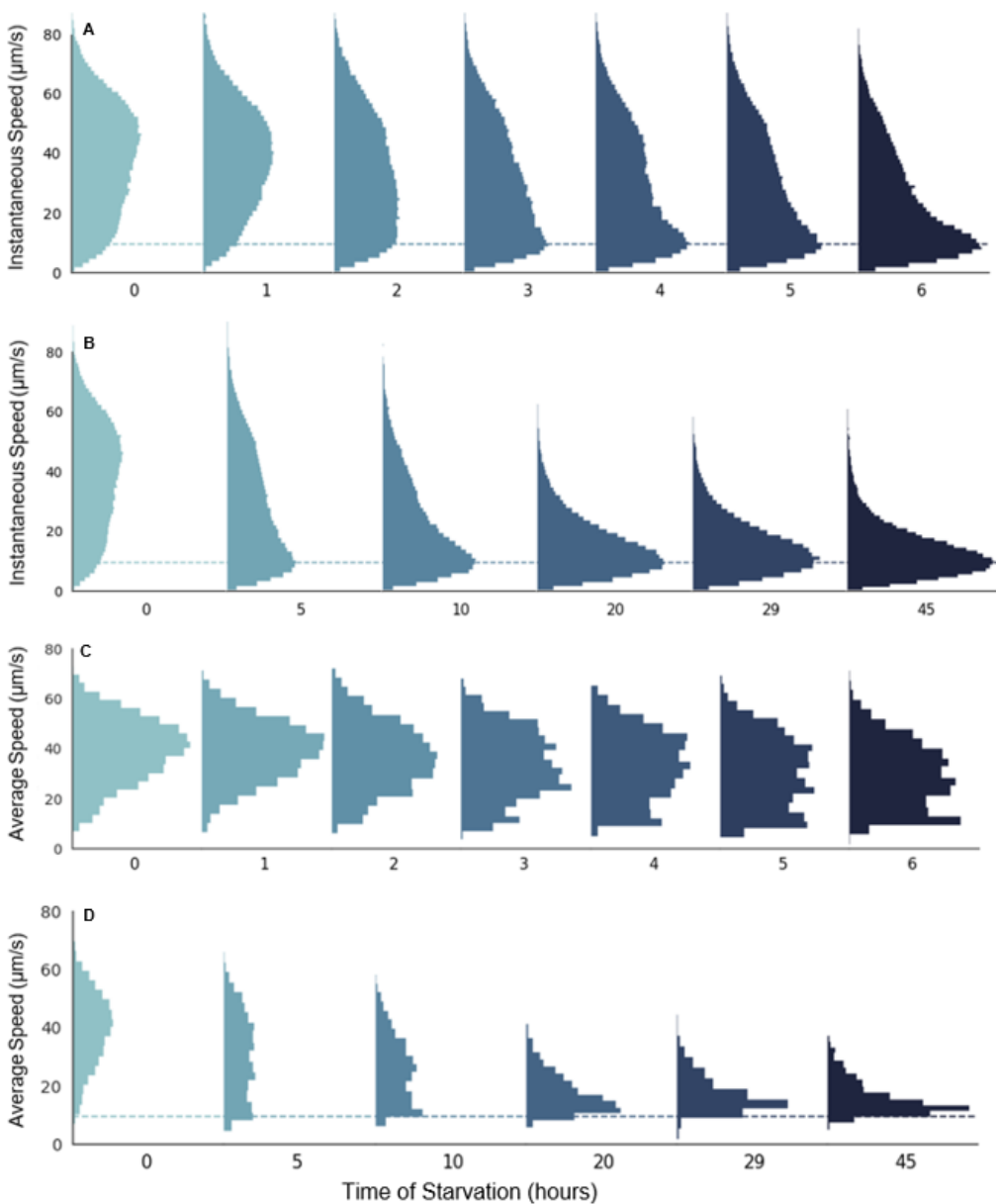
Figure S8: **Under starvation conditions, the instantaneous and average speed distributions of *B. bacteriovorus* shift across time. [run 2].** We follow a similar convention to figure 1 in the main text. The only relevant difference is the number of data points contributing to each histogram. For (A) and (B), the number of instantaneous speed observations ranges from 93,196-172,376; for (C) and (D), the number of average speed observations ranges from 1,327-3,277.
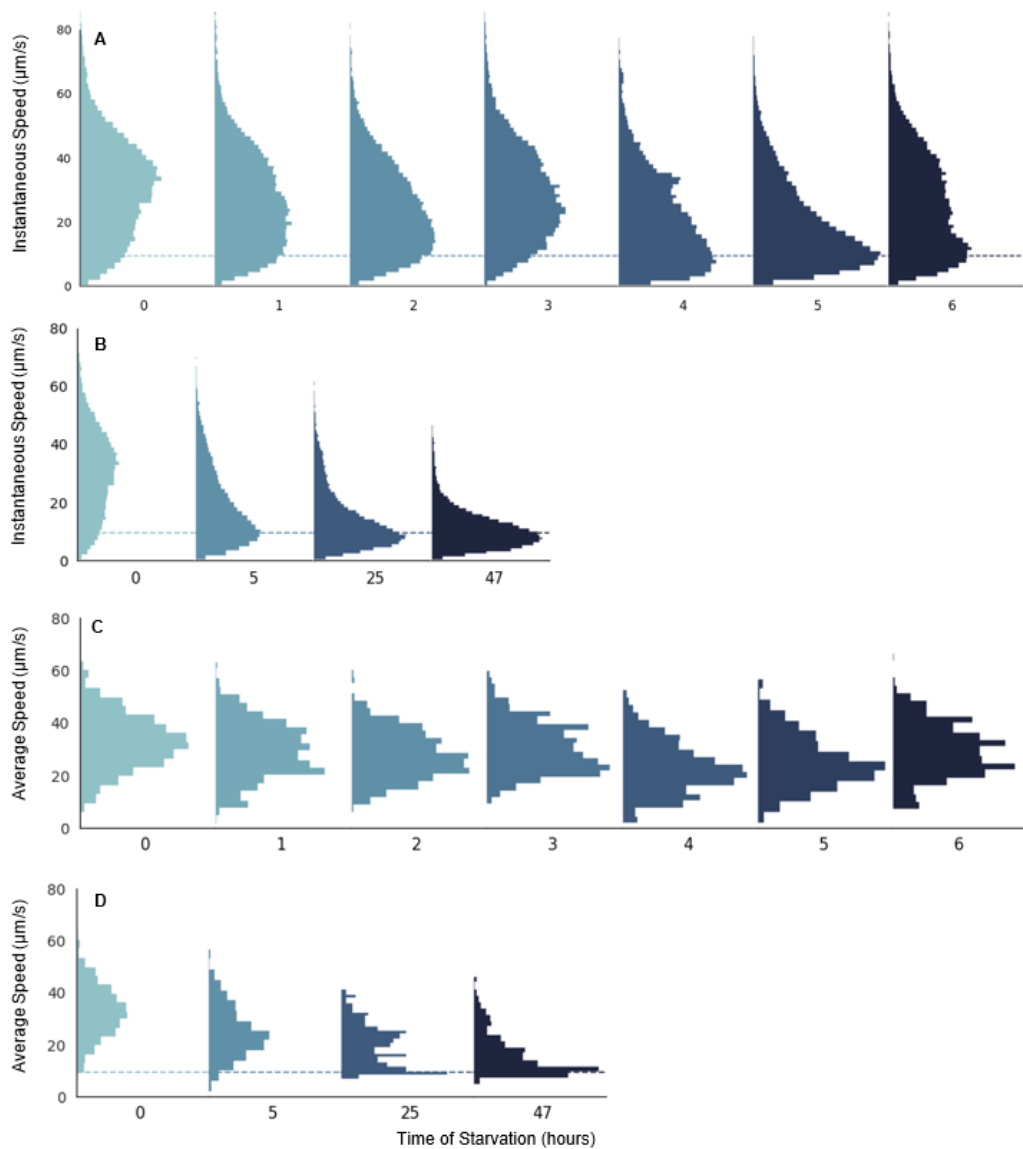
Figure S9: **Under starvation conditions, the instantaneous and average speed distributions of *B. bacteriovorus* shift across time [run 3].** We follow a similar convention to figure 1 in the main text. The only relevant difference is the number of data points contributing to each histogram. For (A) and (B), the number of instantaneous speed observations ranges from 25,959-60,393; for (C) and (D), the number of average speed observations ranges from 247-982.
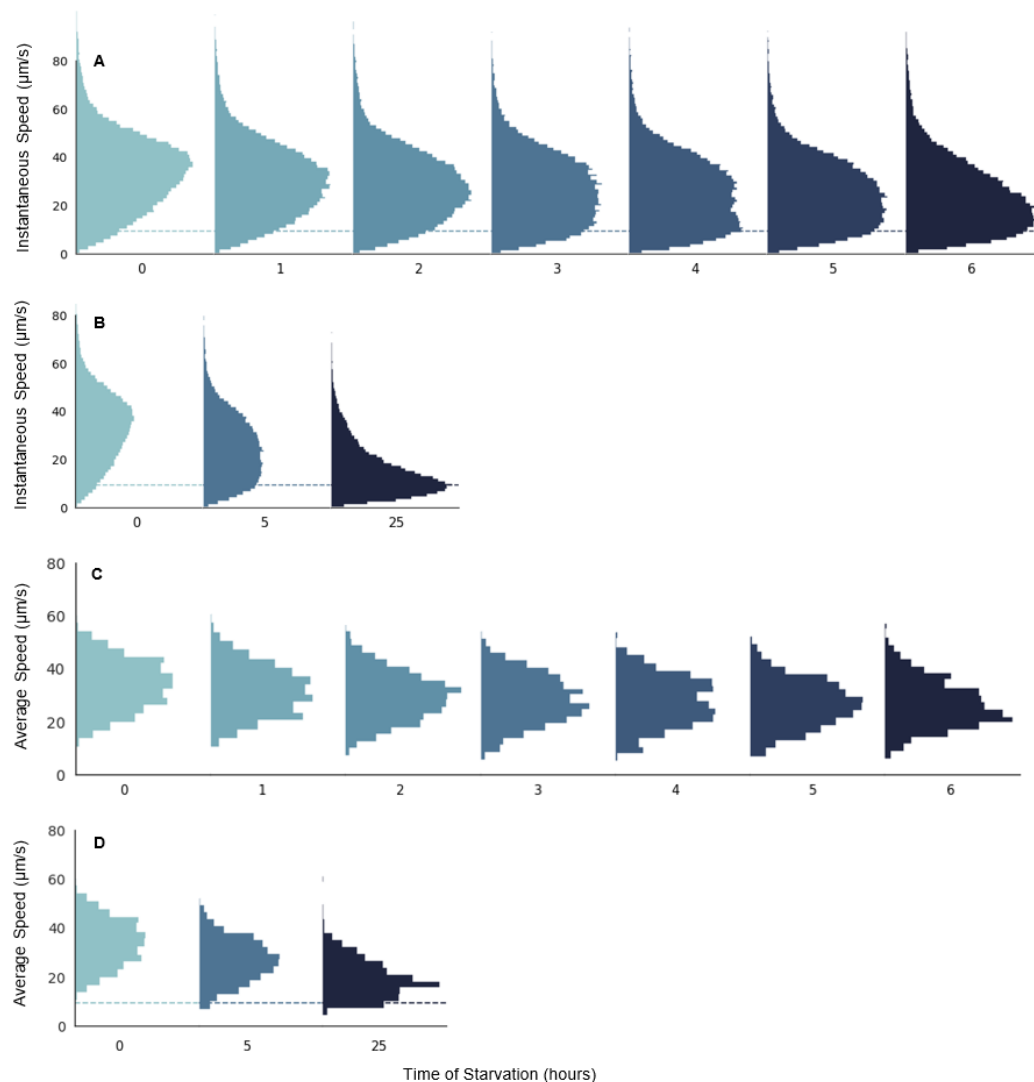
Figure S10: **Under starvation conditions, the instantaneous and average speed distributions of *B. bacteriovorus* shift across time [run 4].** We follow a similar convention to figure 1 in the main text. The only relevant difference is the number of data points contributing to each histogram. For (A) and (B), the number of instantaneous speed observations ranges from 49,264-107,299; for (C) and (D), the number of average speed observations ranges from 500-2,065.

Figure S11: **After addition of LB, *B. bacteriovorus* begins to swim more often even after long starvation times [run 2].** We follow a similar convention to figure 2. The number of instantaneous speed observations ranges from 65,795-110,082 for (A), 84,361-174,041 for (B), 80,625-95,618 for (C), and 141,373-96,026 for (D). Distributions were constructed from 100 evenly spaced bins over the range of instantaneous speed measurements.
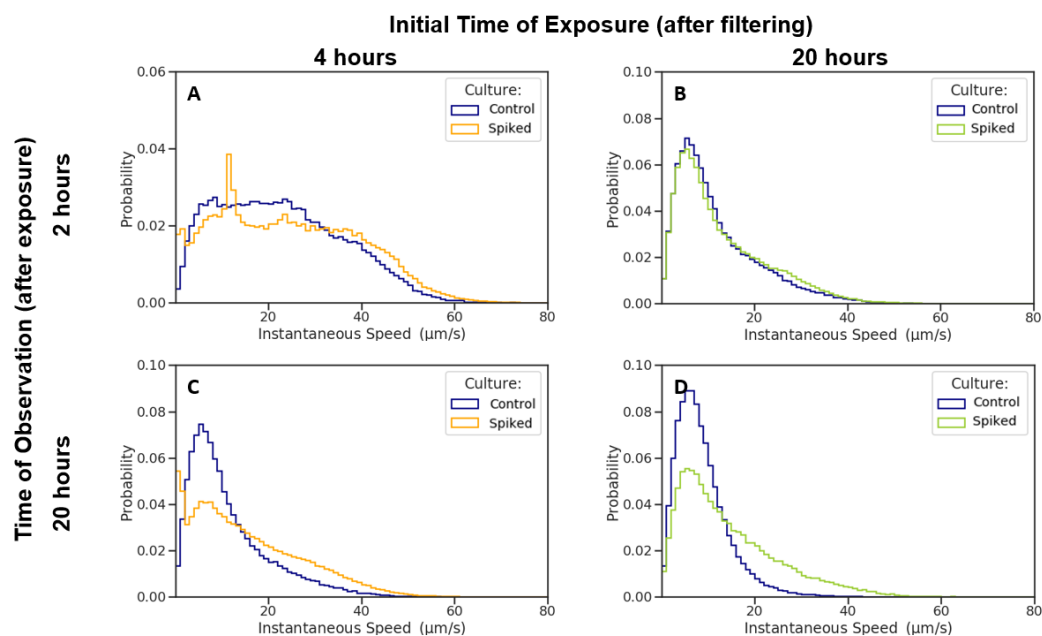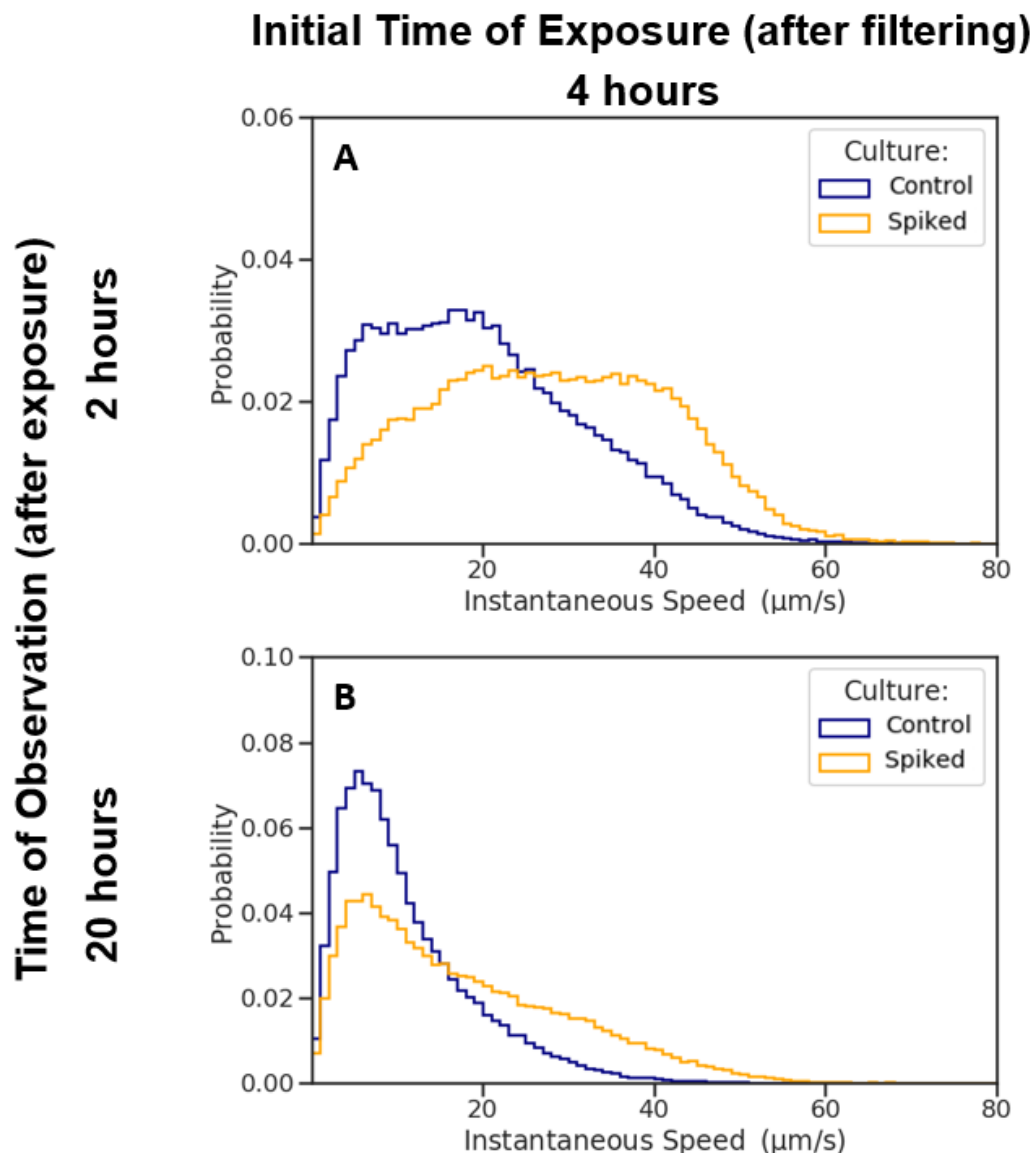
Figure S12: **After addition of LB, *B. bacteriovorus* begins to swim more frequently even after long starvation times [run 3].** We follow a similar convention to figure 2 The number of instantaneous speed observations ranges from 71,290-64,100 for (A) and 68,325-126,841 for (B). Distributions were constructed from 100 evenly spaced bins over the range of instantaneous speed measurements.
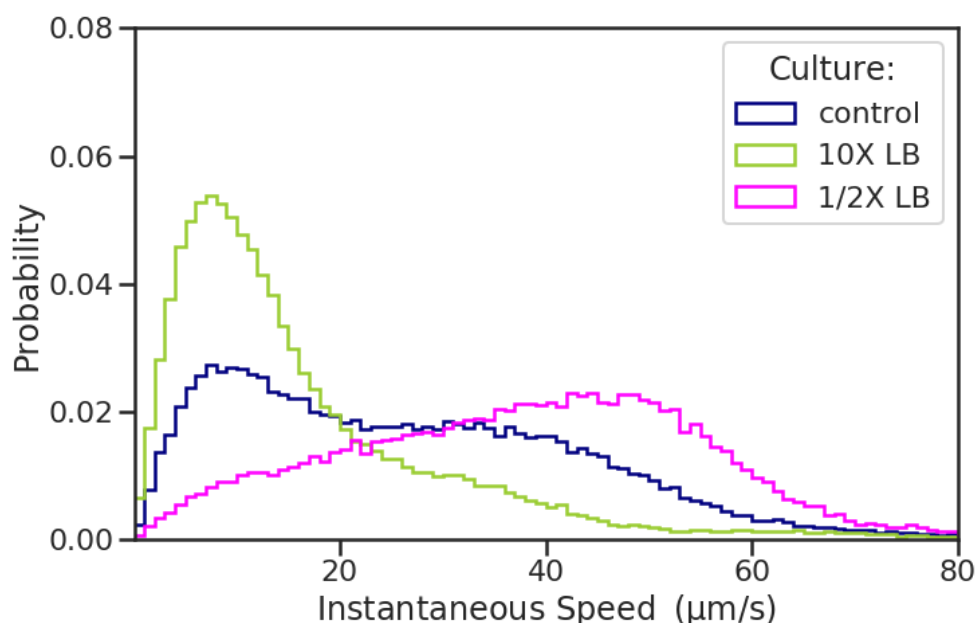
Figure S13: **The speed distributions of spiking experiment is concentration dependent.** A culture starved for four hours and then split into three cultures. One culture remained starving (blue) while the other two were spiked with 10X LB (green) or 1/2X LB concentration (magenta). The culture spiked with the higher concentration resulted in an increase in the apparent diffusive peak whereas the 1/2X culture exhibited an increase in the higher mode peak. This is likely due to an increase in the osmolarity of the solution with the greater concentration of LB. The number of instantaneous speed observations ranges from 49,390-96,644. The data were divided into 100 evenly spaced intervals.

Figure S14: ***B. bacteriovorus* shows no signs of revival after 40 hours of starvation.** We compare the instantaneous speed distributions of our control, starving *B. bacteriovorus* (blue), to that of cultures spiked with LB at Hour 20 (green) and Hour 40 (magenta). Both spiked cultures were observed after 2 hours and 20 hours of exposure. (A) After two hours of exposure, the culture spiked at Hour 20 (green) has faster speeds than the respective control (blue). (B) After two hours of exposure, the culture spiked at Hour 40 has no noticeable change from the control (blue). (C) After 20 hours of exposure, the culture spiked at Hour 20 still has faster instantaneous speeds than the control. (D) After 20 hours of exposure, the culture spiked at Hour 40 has no noticeable change from the control. The number of instantaneous speed observations ranges from 23,472-45,607 for (A), 28,377-79,194 for (B), 46,801-91,407 for (C), and 38,886-84,523 for (D). Distributions were constructed from 100 evenly spaced bins over the range of instantaneous speed measurements.
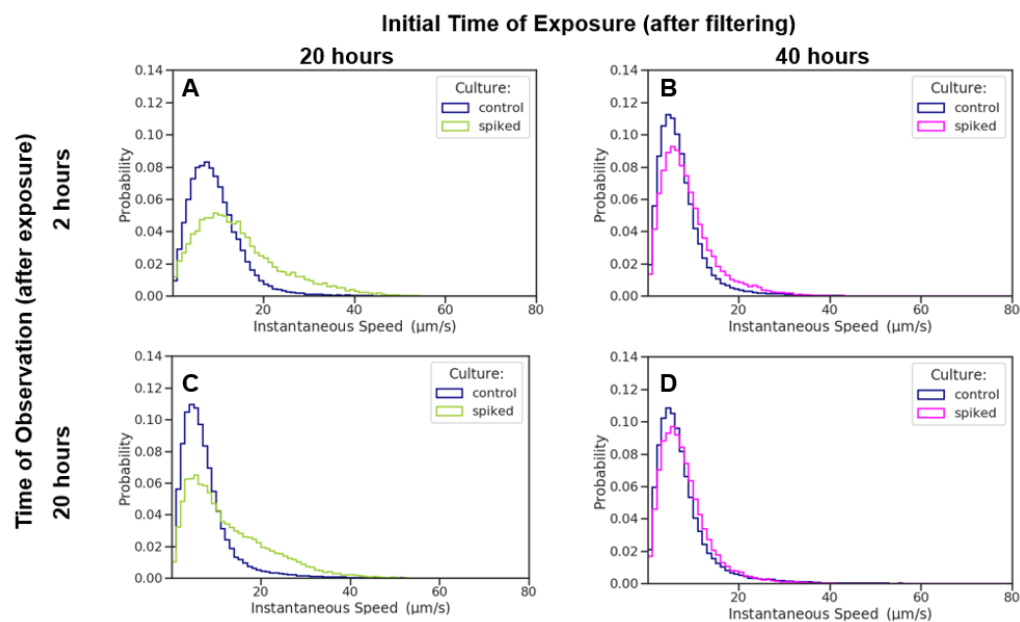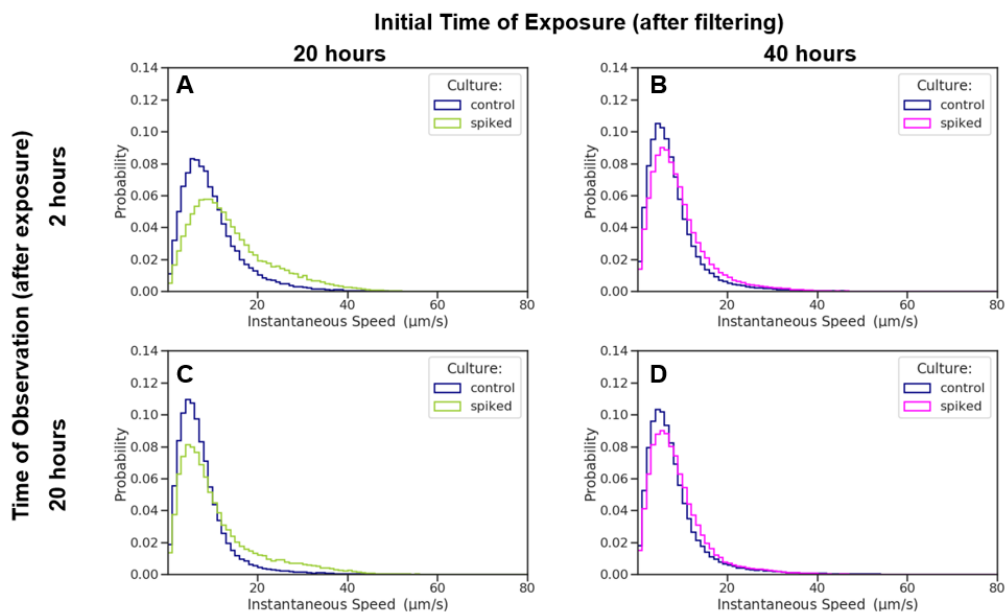
Figure S15: ***B. bacteriovorus* shows no signs of revival after 40 hours of starvation [run 2].** We follow a similar convention to S14. The number of instantaneous speed observations ranges from 36,346-37,567 for (A), 53,562-114,970 for (B), 72,445-110,723 for (C), and 80,017-188,080 for (D). Distributions were constructed from 100 evenly spaced bins over the range of instantaneous speed measurements.

Sampling statistics for main text figures

Figure 1: The area of each histogram is normalized to unity. For (A) and (B), the number of instantaneous speed observations ranges from 65,795-151,604; for (C) and (D), the number of average speed observations ranges from 621-2,589. Instantaneous speed distributions were constructed from 50 evenly spaced bins over the range of instantaneous speed measurements; average speed distributions were constructed from 30 evenly spaced bins over the range of average speed measurements.

Figure 2: The area of each histogram is normalized to unity. The number of instantaneous speed observations ranges from 39,244-39,862 for (A), 29,943-30,707 for (B), 18,841-20,320 for (C), and 56,115-60,393 for (D). Distributions were constructed from 100 evenly spaced bins over the range of instantaneous speed measurements.

Table S1: **Speeds measured at bounding frames after removal of *n* edge frames.**

Bounding frames	Number of frames removed from edge					
	0	**1**	**2**	**3**	**4**	**5**
$< 30\,\mu\mathrm{m\,s}^{-1}$	4303 (55%)	3310 (43%)	*2885 (37%)*	2921 (38%)	2976 (38%)	3039 (39%)
$> 30\,\mu\mathrm{m\,s}^{-1}$	3464 (45%)	4457 (57%)	*4882 (63%)*	4846 (62%)	4791 (62%)	4728 (61%)
Total	7767 (100%)	7767 (100%)	*7767 (100%)*	7767 (100%)	7767 (100%)	7767 (100%)

Speeds measured at the beginning or end of a trajectory are biased towards lower speeds because bacteria moving into or out of focus are more likely to have a *z*-component to their velocity while motion occurs in the *xy*-plane. To determine the degree of bias, between 0 and 5 *edge frames* were trimmed from the beginning and end of all trajectories and the speeds re-measured for the three bounding frames (at the beginning and end of each trajectory). The number (and percentage) of samples above and below $30\,\mu\mathrm{m\,s}^{-1}$ are counted after trimming a given number of edge frames. Removing roughly two edge frames (emphasized above) is sufficient to compensate for the slow speed bias at the ends of trajectories; the percentage of slow speed samples settles around 38%.
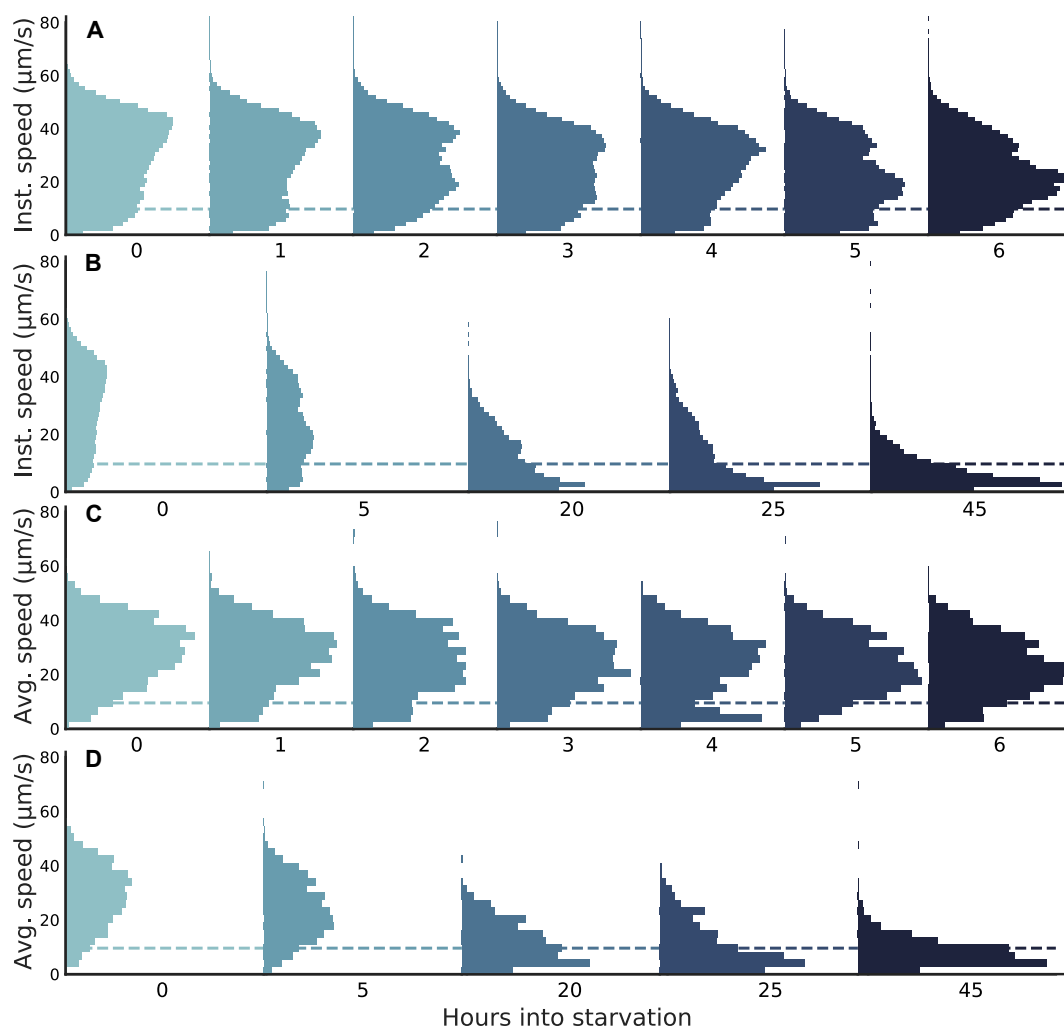
Figure S16: **Recreation of figure 1 with parameter free inference.**

Comparison to another analysis method

To confirm that our results are independent of the analysis method we performed the same localization and tracking analysis using a different framework. For this secondary analysis method we annotated roughly 1000 images by hand, then trained a neural network (based on MMDetection (1)) to automate the remaining localizations. The mean error between hand annotated localizations and neural net localizations was roughly 4 pixels, as seen in figure S3, which is small considering the average width of a *B. bacteriovorus*' diffraction pattern is around 10 pixels (see figure S3). We linked localizations across frames using TrackPy (2). In order to smooth the linked localizations (*i.e.*, tracks), we used a Gaussian process with a squared exponential kernel (3). The parameters of the kernel were then determined by maximizing the likelihood of the trajectory assuming a Gaussian emission model for the localization error.

Figure S16 shows the results of our inference on the same data as in figure 1. As seen in figure S16 we recover a speed histogram that closely matches that of figure 1. In particular the bimodal behavior is evident in both figures. We note however that the secondary analysis method underestimates the speed in the later experimental hours (> 20 hours of starvation). This is because, in the absence of movement the Gaussian process smoothing averages over the stochastic Brownian motion resulting in a speed distribution close to zero. For this reason, we only use this inference to validate the bimodality of the speed histograms, and we use the window average smoothing method explained in the Methods section for the core of our analysis.

In order to further demonstrate the bimodality of *B. bacteriovorus*, we performed a Gaussian mixture fitting on the results of instantaneous speed, as shown in Table S2. The fitting results for the distributions of instantaneous speed during Hours 0-6 revealed two consistent means, approximately $14 \, \mu\mathrm{m\,s}^{-1}$ and $35 \, \mu\mathrm{m\,s}^{-1}$. Furthermore, the weight of the faster speed increased from Hour 0 to Hour 6. After a 20-hour period of starvation, our fitting results indicated that the mean value of $35 \, \mu\mathrm{m\,s}^{-1}$ was no longer present.

Table S2: **Instantaneous speed distributions at different Hours fitted by Gaussian mixtures.**

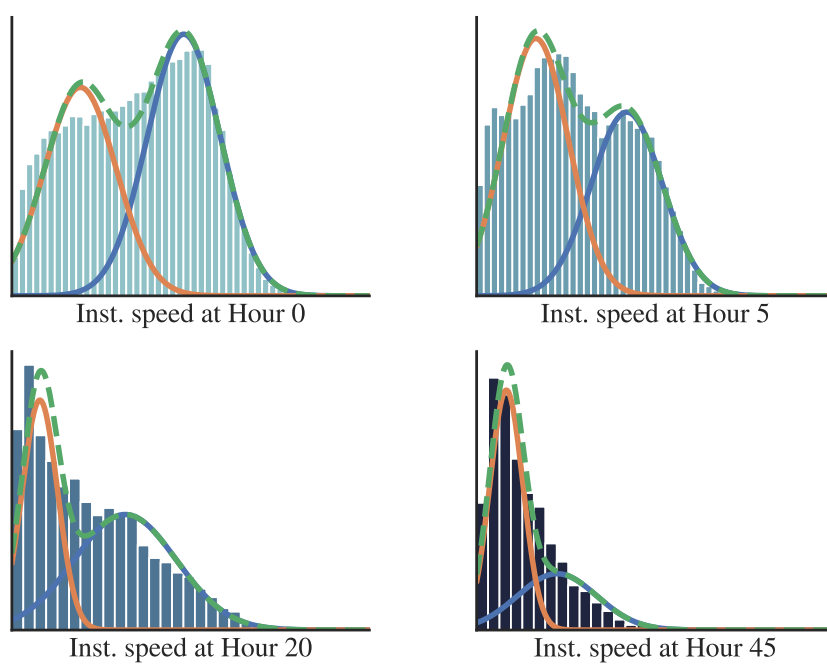| Hour	0	1	2	3	4
Weights	0.440, 0.560	0.427, 0.573	0.508, 0.492	0.479, 0.521	0.437, 0.563
Means ($\mu\mathrm{ms}^{-1}$)	15.3, 38.5	13.7, 36.5	15.7, 37.1	13.7, 34.2	13.9, 33.9
Variances ($\mu\mathrm{m}^2\mathrm{s}^{-2}$)	65.1, 67.3	57.5, 66.1	59.0, 62.1	52.4, 63.2	58.6, 61.5
Hour	5	6	20	25	45
Weights	0.565, 0.435	0.591, 0.409	0.408, 0.592	0.420, 0.580	0.648, 0.352
Means ($\mu\mathrm{ms}^{-1}$)	13.3, 33.7	15.0, 33.4	3.91, 15.8	3.59, 17.2	4.20, 11.3
Variances ($\mu\mathrm{m}^2\mathrm{s}^{-2}$)	53.8, 63.4	54.0, 66.9	6.17, 51.4	4.90, 73.7	5.52, 31.0

Figure S17: **Gaussian mixture fitting discussed in table S2 visualized at some represent times.** The orange and blue curves represent the probability density functions (PDFs) of the individual Gaussian components, while the green dashed curve represents the overall PDF.

SUPPORTING REFERENCES

1. MMDetection Contributors. *OpenMMLab Detection Toolbox and Benchmark*. 2018. URL: https://github.com/open-mmlab/mmdetection.

2. Dan Allan et al. *soft-matter/trackpy: Trackpy v0.4.2*. Version v0.4.2. 2019. DOI: 10.5281/zenodo.3492186.

3. Christopher KI Williams and Carl Edward Rasmussen. *Gaussian processes for machine learning*. Vol. 2. 3. MIT press Cambridge, MA, 2006.